

Anisotropy of transient photoconductivity in functionalized pentacene single crystals

O. Ostroverkhova,^{a)} D. G. Cooke, and F. A. Hegmann

Department of Physics, University of Alberta, Edmonton, Alberta T6G 2J1, Canada

R. R. Tykwinski

Department of Chemistry, University of Alberta, Edmonton, Alberta T6G 2G2, Canada

S. R. Parkin and J. E. Anthony

Department of Chemistry, University of Kentucky, Lexington, Kentucky 40506-0055

(Received 2 May 2006; accepted 25 September 2006; published online 10 November 2006)

We report on the anisotropy of transient photoconductivity in functionalized pentacene single crystals using ultrafast optical pump–terahertz probe techniques. Functionalized pentacene crystals with tri-isopropylsilylethynyl (TIPS) and tri-ethylsilylethynyl (TES) side groups were studied, characterized by crystal structures favoring two-dimensional and one-dimensional charge transports, respectively. Charge carrier mobility anisotropies in the a - b plane of 3.5 ± 0.6 and 12 ± 6 were obtained in the TIPS and TES crystals, respectively, consistent with the degree of π overlap along different directions in the crystals. A photogeneration efficiency anisotropy was also observed in both types of crystals. © 2006 American Institute of Physics. [DOI: 10.1063/1.2387135]

Organic semiconductors have attracted considerable attention due to their potential applications in thin film transistors, organic light-emitting diodes, solar cells, etc.¹ Thin single crystal platelets and polycrystalline thin films are particularly interesting for applications due to their high charge carrier mobilities.^{2,3} However, since the charge transport in organic crystals is highly anisotropic,^{3–5} it is important to know the direction(s) along which mobility is the highest. Although a number of experimental and theoretical studies have addressed mobility anisotropy in organic crystals,^{3–7} its measurement remains challenging. For applications that rely on photoconductivity, it is important to consider that not only mobility but also charge carrier photogeneration efficiency is anisotropic.⁸

Traditional photoconductivity measurements, such as performed in recent studies with pentacene,⁹ functionalized pentacene,¹⁰ and rubrene single crystals,¹¹ require contacts to be made to the sample, making it difficult to probe anisotropy. Ultrafast terahertz pulse techniques, on the other hand, offer the advantage of *noncontact* probing of charge carrier photogeneration and transport on subpicosecond time scales,^{12–15} which makes them valuable in studies of transient photoconductivity anisotropy.¹⁵ In this letter, we use noncontact optical pump–terahertz probe techniques to study the anisotropy of the charge carrier mobility and photogeneration efficiency in the a - b plane of two different modifications of functionalized pentacene single crystals.

In our studies, we used single crystals of pentacene functionalized with (i) 6,13-bis(tri-isopropylsilylethynyl) (TIPS) and (ii) 6,13-bis(triethylsilylethynyl) (TES) side groups [Fig. 1(a)].^{7,16–18} The single crystals were grown in a saturated tetrahydrofuran solution at 4 °C and had dimensions typically around $(1.5–2) \times (2–4)$ mm², as illustrated in Fig. 1(b), with a thickness of 300–500 μ m. Although both TIPS and TES crystals are triclinic (with the unit cell parameters

listed in Table I), the molecular packing and resulting π overlap in these crystals is different, as the TIPS crystals assume a more two-dimensional (2D) “brick-wall-type” structure, while the TES crystals exhibit a one-dimensional (1D) “slipped-stack-type” structure [Figs. 1(c) and 1(d), respectively].^{7,16,18} Our crystallographic analysis showed that the largest area crystal surface corresponds to the a - b plane of the crystals, with the a axis parallel (\parallel) to the long axis in both TIPS and TES crystals. TIPS and TES crystals have almost identical absorption spectra in solution, with the absorption edge at around 700 nm, which shifts to \sim 850 nm in a crystal.¹⁴ Eight TIPS and four TES crystals were studied.

A detailed description of the optical pump–terahertz probe experimental setup used in our studies can be found elsewhere.^{14,15} All experiments were carried out at room temperature. The samples were excited with 100 fs pump pulses at wavelengths of 800, 400, or 580 nm, obtained from an amplified Ti:sapphire laser source (1.08 kHz). Both the terahertz probe and optical pump pulses were at normal incidence to the a - b plane of the single crystal samples. The optically induced negative differential transmission of the

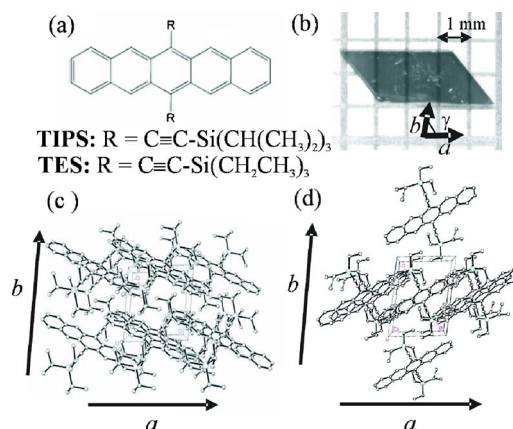


FIG. 1. (a) Molecular structure of TIPS and TES derivatives. (b) Typical TIPS crystal. Molecular packing in (c) TIPS and (d) TES crystals.

^{a)}Present address: Department of Physics, Oregon State University, OR 97331-4501; electronic mail: oksana@science.oregonstate.edu

TABLE I. Crystallographic unit cell parameters and charge carrier mobilities in the a - b plane for the TIPS and TES crystals. Parameters are defined in the text. Angles φ_1 and φ_2 are defined in Fig. 2(a). Since $\eta \leq 1$, the $\eta\mu_{aa}$ values represent a lower limit of the charge carrier mobility along the a axis in TIPS and TES crystals.

| | a (Å) | b (Å) | c (Å) | α (deg) | β (deg) | γ (deg) | $\eta\mu_{aa}$ [cm ² /(V s)] | μ_{aa}/μ_{bb} | μ_{11}/μ_{22} | φ_1 (deg) | φ_2 (deg) |
|------|---------|---------|---------|----------------|---------------|----------------|--|---------------------|---------------------|-------------------|-------------------|
| TIPS | 7.565 | 7.75 | 16.835 | 89.15 | 78.42 | 83.63 | 0.15–0.2 | 3.2±0.5 | 3.5±0.6 | −14 | 76 |
| TES | 7.204 | 9.994 | 11.326 | 80.81 | 89.13 | 82.21 | 0.05–0.06 | 8±3 | 12±6 | 0 | 90 |

terahertz peak amplitude [$-(T-T_0)/T_0 \equiv -\Delta T/T_0$, where T_0 is the amplitude of the terahertz pulse transmitted through the unexcited sample] was monitored as a function of terahertz probe delay time with respect to the optical pump pulse and is proportional to the transient photoconductivity induced in the sample. From the peak value of the transient signal, the product of the charge carrier mobility μ and charge carrier photogeneration efficiency η can then be calculated, as described in Ref. 14.

The $-\Delta T/T_0$ transients observed in the TIPS and TES crystals have very similar shapes and exhibit subpicosecond charge photogeneration and power-law decay dynamics.¹⁴ The $\mu\eta$ product, calculated from the peak of the $-\Delta T/T_0$ transient obtained with the electric field of the terahertz probe pulse (E_{THz}) and that of the optical pump pulse (E_{pump}) parallel to the a axis, yielded ~ 0.15 – 0.2 and ~ 0.05 – 0.06 cm²/(V s) in TIPS and TES crystals, respectively, depending on the sample. Since $\eta \leq 1$,¹⁴ these numbers represent lower limits for the charge carrier mobility along the a axis. Although band-structure calculations predict higher mobilities in functionalized pentacene crystals with the structure supporting 1D charge transport (such as TES) compared to those in crystals supporting 2D charge transport (such as TIPS),⁷ it has been suggested that intermolecular electronic coupling plays an important role in oligoacenes,¹⁸ which complicates the relationship between the crystal structure and the electronic transport. In particular, the TIPS-based organic thin film transistors exhibited much higher field-effect transistor mobilities than TES-based ones,¹⁷ in qualitative agreement with our studies.

The triclinic symmetry group of TIPS and TES crystals leads to a complex picture of charge transport described by six components of the mobility tensor μ_{ij} , where $i, j = x, y, z$ are components in an orthogonal coordinate system (choice of which is somewhat arbitrary), and $\mu_{ij} = \mu_{ji}$.^{4,6} Also, the photogeneration efficiency η is anisotropic in the a - b plane due to the crystal orientation-dependent competition between free charge carrier and exciton generation.⁸ Since in our experiment we cannot separate the mobility and photogeneration efficiency, we performed two types (1 and 2) of experiments in order to differentiate between the a - b -plane anisotropy of the mobility and of the photogeneration efficiency.

Type 1: Anisotropy of mobility. In these experiments, the crystal is rotated in the azimuthal (a - b) plane, so that the angle (φ) between the direction of E_{THz} and the a axis of the crystal changes (at $\varphi = 0^\circ$ E_{THz} is parallel to the a axis). The polarization of the pump (E_{pump}) is rotated with the crystal using a half-wave plate and a polarizer combination in order to maintain E_{pump} parallel to the a axis and ensure the same fluence at all angles. At every angle, the peak value of $-\Delta T/T_0$ is measured and the $\mu\eta$ product is calculated. In this case, the observed angular dependence of the photoconduc-

tivity is purely due to that of the charge carrier mobility. Figures 2(a) and 2(b) show the angular dependence of the charge carrier mobility (averaged over all samples measured at 800, 400, and 580 nm excitation) normalized to the value at $\varphi = 0^\circ$ in TIPS and TES crystals, respectively. The charge carrier mobility along a certain direction $l = (l_i, l_j, l_k)$ is given by $\mu_{ll} = \mu_{ij} l_i l_j$.⁴ For convenience, we choose the orthogonal coordinate system (x, y, z) so that $x \parallel a$ axis, $y \perp x$ and is in the a - b plane, and $z \perp a$ - b plane. Then, in the a - b plane, $l = (\cos \varphi, \sin \varphi, 0)$, and the mobility along l is $\mu_{ll} = \mu_{xx} (\cos \varphi)^2 + \mu_{yy} (\sin \varphi)^2 + \mu_{xy} \sin(2\varphi)$. For example, the mobility along the a axis is $\mu_{aa} = \mu_{xx}$. The equation above normalized by μ_{xx} is used to fit the data in Fig. 2 and yields $\mu_{yy}/\mu_{xx} = 0.34 \pm 0.05$ (0.09 ± 0.05) and $\mu_{xy}/\mu_{xx} = -0.17 \pm 0.04$ (0.06 ± 0.04) in TIPS (TES). Using these components and substituting $\varphi = \gamma$ (for μ_{bb}) in the fit equation, we obtain the ratio of the mobilities along the a and b axes (μ_{aa}/μ_{bb} ,

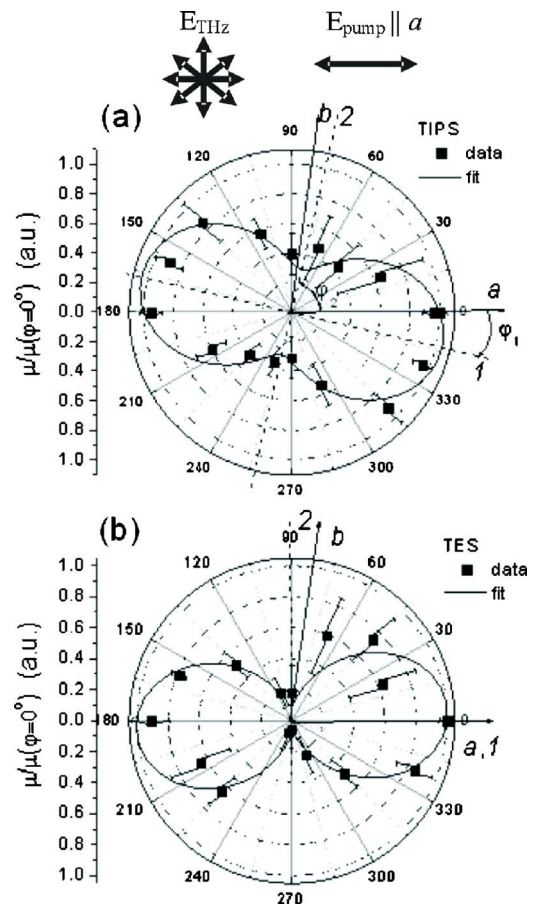


FIG. 2. Dependence of the charge carrier mobility on the azimuthal angle φ obtained in (a) TIPS and (b) TES crystals. In both crystals, $\varphi = 0^\circ$ corresponds to the a axis. Lines correspond to the fit with a function described in the text. Crystallographic a and b axes as well as the principal axes 1 and 2 are also shown.

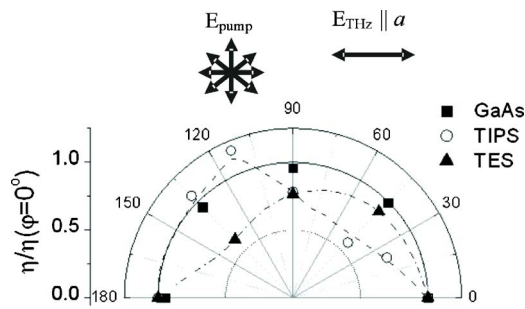


FIG. 3. Dependence of the free charge carrier photogeneration efficiency at 800 nm on the angle between the optical pump polarization and a axis. Data for GaAs, TIPS, and TES are shown (symbols). Lines represent guides for the eyes.

Table I). Assuming that μ_{yz} and μ_{xz} components of the mobility tensor are small,⁶ we diagonalize the x - y part of the tensor and determine the directions of the principal axes 1 and 2, as well as the corresponding mobilities μ_{11} ($1.04\mu_{aa}$ and $1.004\mu_{aa}$ in TIPS and TES, respectively) and μ_{22} ($0.30\mu_{aa}$ and $0.086\mu_{aa}$ in TIPS and TES, respectively), whose ratio μ_{22}/μ_{11} yields 3.5 ± 0.6 and 12 ± 6 for TIPS and TES, respectively (Table I). The mobility anisotropy of 3.5 in the TIPS crystal is very similar to that obtained in rubrene³ and pentacene⁵ single crystals using a field-effect transistor geometry. Considerable difference in the in-plane mobility anisotropy between the TIPS and TES crystals supports a theoretical prediction of much stronger mobility anisotropy in the case of the TES-type crystals that favor 1D charge transport based on the crystal structure and molecular packing [Figs. 1(c) and 1(d)].^{7,16,18} In TIPS, the principal axes 1 and 2 constitute angles $\varphi_1 = -14^\circ$ and $\varphi_2 = 76^\circ$ with respect to the a axis, respectively [Fig. 2(a)]. Interestingly, the highest mobility axis does not exactly coincide with the direction of maximum π overlap along the a axis [Fig. 1(c) and Ref. 16], which highlights the contribution of factors unrelated to band structure, such as fluctuations of the intermolecular coupling,¹⁸ to charge carrier mobility in organic molecular crystals. In TES, the principal (highest mobility) axis 1 is coincident with the direction of maximum π overlap along the a axis [Figs. 1(d) and 2(b)]. However, it is possible that due to the above mentioned fluctuations in the observed in-plane anisotropy of ~ 12 [Fig. 2(b) and Table I] is smaller than that expected based solely on the band structure.⁷ Mobility anisotropy, a signature of bandlike transport in organic molecular crystals,³ is consistent with our previous claim of bandlike transport in functionalized pentacene single crystals.¹⁴

Type 2: Anisotropy of the photogeneration efficiency. In these experiments, E_{THz} is kept parallel to the a axis of the crystal, while E_{pump} is rotated in the azimuthal plane, so that the angle (φ) between the E_{pump} and the a axis changes (at $\varphi=0^\circ$, $E_{\text{pump}}\parallel a$ axis). Thick crystals were chosen to ensure that the light at all wavelengths used in our study was fully absorbed, regardless of the polarization. Taking into account that the terahertz pulse probes the conductivity across the entire thickness the angular dependence of the transient photoconductivity in this case is due to that of the photogeneration efficiency η . Figure 3 illustrates angular dependence of the photogeneration efficiency normalized to its value at $\varphi=0^\circ$ in TIPS and TES crystals (averaged over all samples) obtained with 800 nm excitation. As a control sample, we

used a semi-insulating GaAs sample excited at 800 nm (also included in Fig. 3), which exhibits an isotropic photogeneration efficiency ($\eta(\varphi)/\eta(\varphi=0^\circ)\approx 1$ within $\sim 5\%$) as expected. a - b -plane anisotropies for η of about 1.7 and 2 are observed at 800 nm in the TIPS and TES crystals, respectively. At 800 nm, the most efficient charge photogeneration occurs when E_{pump} is at $\varphi\sim 115^\circ$ (Fig. 3) with respect to the a axis in the case of TIPS and when $E_{\text{pump}}\parallel a$ axis in the case of TES. The shape of the distribution in Fig. 3 depends on the wavelength of optical excitation and has to be separately determined for each wavelength. For example, in TIPS crystals, the ratios of $\eta(\varphi=90^\circ)/\eta(\varphi=0^\circ)$ are approximately 0.8, 0.47, and 0.95 at the wavelengths of 800, 580, and 400 nm, respectively.

In summary, we observed anisotropy in both the charge carrier mobility and photogeneration efficiency in two types of functionalized pentacene single crystals. The highest mobility direction was consistent with the direction for the highest degree of π overlap in the crystals. Mobility anisotropy factors of 3.5 ± 0.6 and 12 ± 6 are observed in TIPS and TES crystals whose structure supports 2D and 1D charge transport, respectively.

The authors thank V. Podzorov for helpful discussions. This work was supported by NSERC, CIPI, ONR, iCORE, and the Killam Trust.

¹S. R. Forrest, *Nature (London)* **428**, 911 (2004).

²M. M. Payne, S. R. Parkin, J. E. Anthony, C. C. Kuo, and T. N. Jackson, *J. Am. Chem. Soc.* **127**, 4986 (2005); O. D. Jurchescu, J. Baas, and T. T. M. Palstra, *Appl. Phys. Lett.* **84**, 3061 (2004).

³V. Podzorov, E. Menard, A. Borissov, V. Kiryukhin, J. A. Rogers, and M. E. Gershenson, *Phys. Rev. Lett.* **93**, 086602 (2004).

⁴N. Karl, in *Organic Electronic Materials*, edited by R. Farchioni and G. Grosso (Springer, New York, 2001).

⁵J. Y. Lee, S. Roth, and Y. W. Park, *Appl. Phys. Lett.* **88**, 252106 (2006).

⁶D. A. da Silva, E. G. Kim, and J. L. Brédas, *Adv. Mater. (Weinheim, Ger.)* **17**, 1072 (2005); K. Hannewald and P. A. Bobbert, *Phys. Rev. B* **69**, 075212 (2004).

⁷R. C. Haddon, X. Chi, M. E. Itkis, J. E. Anthony, D. L. Eaton, T. Siegrist, C. C. Mattheus, and T. T. M. Palstra, *J. Phys. Chem. B* **106**, 8288 (2002).

⁸M. Pope and C. E. Swenberg, *Electronic Processes in Organic Crystals and Polymers*, 2nd ed. (Oxford University Press, New York, 1999), Vol. 56, p. 1328.

⁹D. V. Lang, X. Chi, T. Siegrist, A. M. Sargent, and A. P. Ramirez, *Phys. Rev. Lett.* **93**, 086802 (2004); Z. Rang, A. Haraldsson, D. M. Kim, P. P. Ruden, M. I. Nathan, R. J. Chesterfield, and C. D. Frisbie, *Appl. Phys. Lett.* **79**, 2731 (2001).

¹⁰T. Tokomuto, J. S. Brooks, R. Clinite, X. Wei, J. E. Anthony, D. L. Eaton, and S. R. Parkin, *J. Appl. Phys.* **92**, 5208 (2002).

¹¹H. Najafov, I. Biaggio, V. Podzorov, M. F. Calhoun, and M. E. Gershenson, *Phys. Rev. Lett.* **96**, 056604 (2006).

¹²F. A. Hegmann, O. Ostroverkhova, and D. G. Cooke, in *Photophysics of Molecular Materials*, edited by G. Lanzani (Wiley-VCH, Weinheim, 2005), Vol. XVII, pp. 367–428.

¹³V. K. Thorsmølle, R. D. Averitt, X. Chi, D. J. Hilton, D. L. Smith, A. P. Ramirez, and A. J. Taylor, *Appl. Phys. Lett.* **84**, 891 (2004).

¹⁴O. Ostroverkhova, D. G. Cooke, S. Shcherbyna, R. F. Egerton, F. A. Hegmann, R. R. Tykwinski, and J. E. Anthony, *Phys. Rev. B* **71**, 035204 (2005); O. Ostroverkhova, S. Shcherbyna, D. G. Cooke, R. F. Egerton, F. A. Hegmann, R. R. Tykwinski, S. R. Parkin, and J. E. Anthony, *J. Appl. Phys.* **98**, 033701 (2005).

¹⁵D. G. Cooke, F. A. Hegmann, Y. I. Mazur, W. Q. Ma, X. Wang, Z. M. Wang, G. J. Salamo, M. Xiao, T. D. Mishima, and M. B. Johnson, *Appl. Phys. Lett.* **85**, 3839 (2004).

¹⁶J. E. Anthony, D. L. Eaton, and S. R. Parkin, *Org. Lett.* **4**, 15 (2002).

¹⁷C. D. Sheraw, T. N. Jackson, D. L. Eaton, and J. E. Anthony, *Adv. Mater. (Weinheim, Ger.)* **15**, 2009 (2003).

¹⁸A. Troisi, G. Orlandi, and J. E. Anthony, *Chem. Mater.* **17**, 5024 (2005).